A PARAMETRIC STUDY ON MELTING AND RESOLIDIDICATION OF A TWO-COMPONENT METAL POWDER LAYER ON TOP OF THE SINTERED METAL POWDER LAYERS

Tiebing Chen and Yuwen Zhang
Department of Mechanical and Aerospace Engineering
University of Missouri-Columbia
Columbia, MO 65211, USA
zhangyu@missouri.edu

ABSTRACT

Selective Laser Sintering (SLS) of a two-component metal powder layer on the top of multiple sintered layers by a moving Gaussian laser beam is modeled. The loose metal powder layer is composed of a powder mixture with significantly different melting points. The physical model which accounts the shrinkage induced by melting is described by using a temperature-transforming model. The effects of the porosity and the thickness of the atop loose powder layer with different numbers of the existing sintered metal powder layers below on the sintering process are investigated numerically. The present work will provide a better understanding to simulate much more complicated three-dimensional SLS process.

NOMENCLATURE

b	moving heat source half width (m)
Bi	Biot number, hb/k_H
C	dimensionless heat capacity, C^0/C_H^0
C^0	heat capacity, ρc_p
c_p	specific heat, ($J/Kg\,K$)
h	convective heat transfer coefficient, ($W/m^2\,K$)
h_m	latent heat of melting or solidification, (J/kg)
I_0	heat source intensity at the center of the heat source, (W/m^2)
k	thermal conductivity, ($W/m\,K$)
K	dimensionless thermal conductivity, k/k_H
N	numbers of sintered layers under the loose powder layer
N_i	dimensionless moving heat source intensity, $\alpha_a I_0 b/[k_H(T_m^0 - T_i^0)]$
N_R	Radiation number, $\varepsilon\sigma(T_m^0 - T_i^0)^3 b/k_H$
N_t	temperature ratio for radiation, $T_m^0/(T_m^0 - T_i^0)$
s	solid-liquid interface location (m)
s_0	location of surface (m)
s_{st}	sintered depth (m)
Sc	subcooling parameter, $C_H^0(T_m^0 - T_i^0)/(\rho_L h_{sl})$
T	dimensionless temperature, $(T^0 - T_m^0)/(T_m^0 - T_i^0)$
t	false time (s)
T^0	temperature (K)
u	heat source moving velocity (m/s)
U	dimensionless heat source moving velocity, ub/α_H
V	volume (m^3)
w	velocity of liquid phase (m/s)
W	dimensionless velocity of the liquid phase, wb/α_H
x	moving horizontal coordinate
X	dimensionless moving horizontal coordinate, x/b
z	vertical coordinate (m)
Z	dimensionless vertical coordinate, z/b

GREEK SYMBOL

α	thermal diffusivity ($m^2\,s^{-1}$)
δ	powder layer thickness,(m)
Δ	dimensionless powder layer thickness, δ/b
ΔT^0	one-half of phase-change temperature range (K)
ΔT	one-half of dimensionless phase change temperature range $(T^0 - T_m^0)/(T_m^0 - T_i^0)$
ε	volume fraction of gas (porosity for unsintered powder), $V_g/(V_g + V_L + V_H)$
ε_e	emissivity of surface
η	dimensionless solid-liquid interface location, s/b
η_0	dimensionless location of the surface, s_0/b
η_{st}	dimensionless sintered depth, s_{st}/b
ρ	density (kg/m^3)
σ	Stefan-Boltzman constant, $5.67\times10^{-8}\,W/(m^2\,K^4)$
τ	dimensionless false time, $\alpha_H t/b^2$
ϕ	volume percentage of low melting point powder, $V_L/(V_L + V_H)$

SUBSCRIPTS

eff	effective
H	high melting point powder
L	low melting point powder

m	melting point
p	sintered parts
s	solid

1. INTRODUCTION

Direct Selective Laser Sintering (SLS) is a process of Solid Freeform Fabrication (SFF) by which 3-D functional parts are built by using CAD data (Conley and Marcus, 1997). A fabricated layer is created by selectively fusing a thin layer of the powder with a scanning laser beam. After sintering of a layer, a new layer of the powder is deposited and sintered in the same manner. A 3-D part is then built by a layer-by-layer process. The single-component powder system investigated in the earlier research is unsuccessful because of the so called "balling" phenomenon which is resulted from the insufficient tensile traction on the molten that leads to the formation of spheres with the approximate diameter of the laser beam, although the recent research showed the "balling" can be avoided by scanning at very high intensity with very small beam spot sizes (Karapatics et al., 1999). The two-component powder approach, which uses two types of the metal powders possessing significantly different melting points, has been used successfully in SLS processing metals (Manzur et al., 1996; Bunnell, 1995) as another way to avoid "balling" phenomenon. The high melting point powders never melt in the sintering process and play a role as the support structure necessary to avoid "balling" in the sintering process. The particular material properties and methods of material analysis of the metal-based powder system for selective laser sintering applications are addressed by Storch et al. (2003).

Melting and resolidification are the mechanisms of metal powder-based SLS to bond powder particles in order to fabricate a functional part. Fundamentals of melting and solidification have been investigated extensively and detailed reviews are available in the literatures (Viskanta, 1983; Yao and Prusa, 1989). During the SLS process of the two-component metal powder system, only the low melting point metal powder goes though melting and resolidification while the high melting point metal powder remains solid in the entire process. Significant density change due to the shrinkage occurs during melting in the sintering process since the high melting point powder alone cannot support the structure of the powder layer when the low melting point powder melts. Zhang and Faghri (1999) analytically solved a one-dimensional melting problem in a semi-infinite powder bed containing a two-component powder mixture subjected to a constant heat flux heating, of which the shrinkage is considered. Chen and Zhang (2003) obtained an analytical solution of one-dimensional melting of the two-component metal powder layer with finite thickness. A two-dimensional steady–state laser-melting problem using an ADI scheme with a false transient formulation was solved by Basu and Srinivasan (1988). A two-dimensional transient model of laser-melting problem with a moving laser beam, of which the interface energy balance was neglect, was developed by Chan et al. (1984). Melting and resolidification of a subcooled semi-infinite two-component metal powder bed with a moving Gaussian heat source was simulated by Zhang and Faghri (1998). They also simulated the three-dimensional sintering process of two-component metal powder with stationary and moving laser beams (2000).

SLS is a process that functional part is fabricated by sintering of the powder layer by layer. References above concern mainly the sintering process in the first loose metal powder layers. The geometry of direct SLS-processed stainless steel layers affected by laser power, scan spacing and scanning speed was investigated by Taylor et al. (2002). The effects of moving laser beam intensity, scanning velocity and numbers of existing sintered layers on the sintering process was simulated by Chen and Zhang (2003). However, the thicknesses of the existing sintered layers and the loose powder were unchanged in this reference. The present paper focuses on the sintering process affected by the change of the thickness of the atop loose powder layer that is located on the top of the multiple existing sintered layers. The formation of the liquid pool in the sintering process will be discussed. The best combination of the processing parameter that allows complete melting of the loose powder and bond with the existing sintered layers are determined numerically.

2. PHYSICAL MODEL

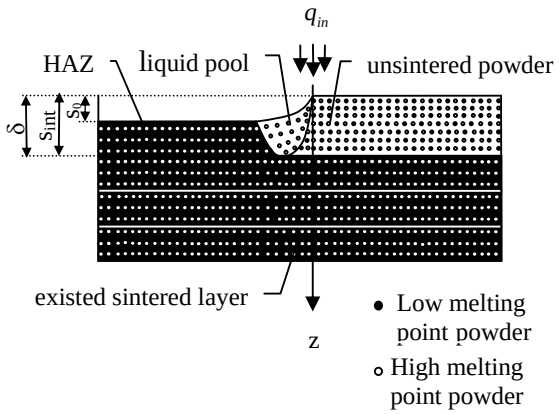

Fig. 1 Physical Model

SLS is a 3-D layer-by-layer process; however, it is a good start point to begin with 2-D model before much more complicated 3-D model is investigated. Figure 1 shows that a two-component metal powder with significantly different melting points is on the top of multiple existing sintered layers. Each existing sintered layer was produced by sintering of the loose metal powder with a scanning laser beam. A laser-induced heat affected zoon (HAZ) of bonded material is formed on top of the existing sintered layers and eventually form a new thin layer of solid part. Melting and resolidification occurring in the sintering process is assumed to be a conduction controlled phase-change problem. The thermal properties of the low melting point powder for

both liquid and solid phases are assumed to be the same. The bottom surface of the computational domain is adiabatic. The initial porosity of the loose metal powder layer is uniform. The porosity of HAZ and existing sintered layers is zero, which means an ideally full densitified layer is achieved after sintering. The horizontal dimension of the computational domain is sufficiently large compared with the diameter of the laser beam so that the problem can be modeled as a quasi-steady-state problem in a coordinate system that is attached to and moves with the laser beam.

The problem is formulated using a temperature transforming model, which converts the enthalpy-based energy equation into a nonlinear equation with a single dependent variable - temperature. In this methodology, the solid-liquid phase change is assumed to occur in a very small range of phase-change temperatures from $(T_m^0 - \delta T^0)$ to $(T_m^0 + \delta T^0)$ (Cao and Faghri, 1990). The beauty of temperature transforming model is that the converged solution can always be obtained without the limitations on grid size and time step for the conduction-controlled phase-change problem. A moving coordinate system, of which the origin is fixed at the center of the heat source and moved together with it at the speed, u , is employed. Therefore, a nonlinear convection term is introduced into the governing equation. The dimensionless governing equation in the moving coordinate system is

$$-U\frac{\partial(CT)}{\partial X}+W\frac{\partial(CT)}{\partial Z}=\frac{\partial}{\partial X}(K\frac{\partial T}{\partial X})+\frac{\partial}{\partial Z}(K\frac{\partial T}{\partial Z})-(-U\frac{\partial S}{\partial X}+W\frac{\partial S}{\partial Z}) \tag{1}$$

where the dimensionless variables are defined in the nomenclature. The dimensionless shrinkage velocity, W , heat capacity, C, source term, S, and thermal conductivity, K , in the region of the atop loose powder layer are different from those in existing sintered layers below, which have been fully densitified. In the region of the loose powder layer,

$$W=\begin{cases}-\varepsilon_s U\dfrac{\partial \eta_{st}}{\partial X} & Z\le\eta_{st}\le\Delta\\ 0 & Z>\eta_{st}\le\Delta\end{cases} \tag{2}$$

$$C=\begin{cases}(1-\varepsilon)(\phi C_L+1-\phi) & T<-\Delta T\\ (1-\varepsilon)(\phi C_L+1-\phi)+(1-\varepsilon)\phi\dfrac{C_L}{2Sc\Delta T} & -\Delta T<T<\Delta T\\ (1-\varepsilon)(\phi C_L+1-\phi) & T>\Delta T\end{cases} \tag{3}$$

$$S=\begin{cases}0 & T<-\Delta T\\ \dfrac{(1-\varepsilon)\phi C_L}{2Sc} & -\Delta T<T<\Delta T\\ \dfrac{(1-\varepsilon)\phi C_L}{Sc} & T>\Delta T\end{cases} \tag{4}$$

$$K=\begin{cases}K_{eff} & T<-\Delta T\\ K_{eff}+\dfrac{K_p-K_{eff}}{2\Delta T}(T+\Delta T) & -\Delta T<T<\Delta T\\ K_p & T>\Delta T\end{cases} \tag{5}$$

In the resolidified region at the left side of liquid pool and the region of the existing sintered layers below,

$$W=0 \tag{6}$$

$$C=(1-\varepsilon)(\phi C_L+1-\phi) \tag{7}$$

$$S=\frac{(1-\varepsilon)\phi C_L}{Sc} \tag{8}$$

$$K=K_p \tag{9}$$

where K_{eff} is the dimensionless effective thermal conductivity of the loose powder region and K_p is dimensionless thermal conductivity in the sintered region. The mathematical descriptions of K_{eff} and K_p are given in Zhang and Faghri (1998). The corresponding boundary conditions of eq. (1) are as following

$$-K\frac{\partial T}{\partial Z}=N_i\exp(-X^2)-N_R[(T+N_t)^4-(T_\infty+N_t)^4]-Bi(T-T_\infty)\quad Z=\eta_0(X) \tag{10}$$

$$\frac{\partial T}{\partial Z}=0,\quad Z=\Delta_s+N\Delta_p,-\infty\le X\le\infty,\quad \tau>0 \tag{11}$$

$$T=-1,\qquad |X|\to\infty,\qquad 0\le Z\le\Delta,\quad \tau>0 \tag{12}$$

The location of liquid surface is related to the sintered depth with the assumption that the sintered layers are fully densitified, i.e.,

$$\eta_0(X)=\varepsilon_s\eta_{st}(X) \tag{13}$$

3. NUMERICAL SOLUTION

The sintering process formulated in the preceding section is a steady-state problem in the moving coordinate system. The energy equation is solved by the false transient method and the converged steady-state solution is declared when the temperature distribution do not vary with the false time. The conduction-convection terms in the energy equation are interpreted by the power-law scheme (Patankar, 1980). The computational domain has an irregular shape which is composed of unsintered powder, liquid pool and sintered region as shown in the physical model due to the shrinkage. A block-off technique (Patankar, 1980) is employed in order to transform the irregular shape of the computational domain due to the shrinkage into the regular shape. The thermal conductivity in the empty space created by the shrinkage is zero.

In order to obtain the quasi-steady-state solution, the computational domain in X direction must be large enough compared with the dimension of moving heat source. The computation was carried out with non-uniform grids both in X and Z directions. The fine grids are distributed around the origin symmetrically in X direction. In Z direction, the grids are distributed uniformly in the loose powder layer but non-uniformly in existing sintered layers by an arithmetic progression. The optimized combination of heat source intensity and scanning velocity is obtained when the sintering depth penetrates the bottom surface of the loose powder layer. In order to trace the sintering depth, a small value of heat source intensity associated with a specific scanning velocity is assigned at first. The value of heat source intensity is increased by a small increment if the sintering depth does not move further at the previous value of the heat source intensity. When the sintering depth approaches very close to the bottom surface of the loose powder layer, the dimensionless increment of the heat source intensity is shifted to a smaller value in order to obtain more accurate solution. The optimized processing parameters are obtained when the sintering depth penetrates the bottom surface of the loose powder layer.

4. RESULTS AND DISCUSSIONS

The thickness of the loose powder layer which is located on the top of the multiple sintered layers is a crucial factor to consider in the modeling since it will affect shape of the induced liquid pool. The sintering processes in the loose powder layer with different thicknesses are simulated when the numbers of existing sintered layers below and scanning velocities of the laser beam were changed.

Figure 2 shows the effect of the different numbers of the existing sintered layers on the sintering process in the atop loose powder layer ($\Delta = 0.25, U = 0.075$). The corresponding optimized laser beam intensities are shown in parentheses. Compared with the sintering process in the loose powder layer with only one sintered layer below, the volume of the liquid pool increases as one more sintered layer is added at the bottom. It is because that the higher laser beam intensity is required in order to achieve the full sintering of the loose powder layer when the number of sintered layers below increases. More heat is lost due to conduction since the dimensionless thermal conductivity of sintered layers is larger than that of the loose powder layer. It can be seen that the shape of the liquid pools is similar when the number of sintered layers below increases. When the sintering depth approaches to the interface between the loose powder layer and the sintered layer, a small protuberant part at the bottom of the liquid pool will reach the interface in advance. Therefore, it is necessary to let the sintering depth go beyond the bottom surface of the loose powder layer slightly in order to bond the newly sintered layer to the existing sintered layer together. Figure 3 shows the effect of the number of existing sintered layers on the sintering process in the loose powder layer as the laser beam scanning velocity increases ($\Delta = 0.25, U = 0.1$). For each case with specific numbers of existing sintered layers, the shape of the liquid pools changes insignificantly with slightly increasing laser beam scanning velocities.

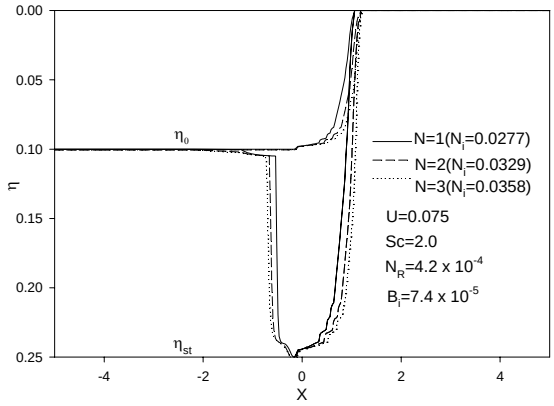

Fig. 2 Effects of numbers of existing sintered layers on the sintering process ($\Delta = 0.25$, $U = 0.075$)

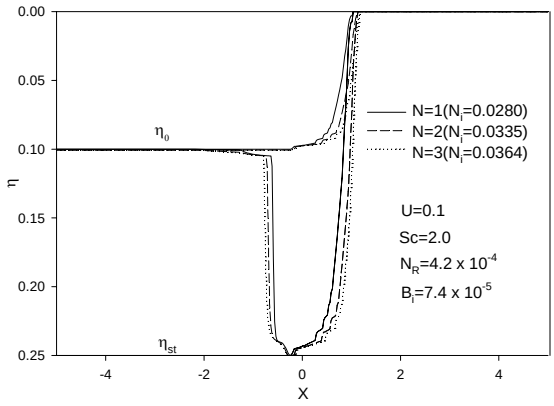

Fig. 3 Effects of numbers of existing sintered layers on the sintering process ($\Delta = 0.25$, $U = 0.1$)

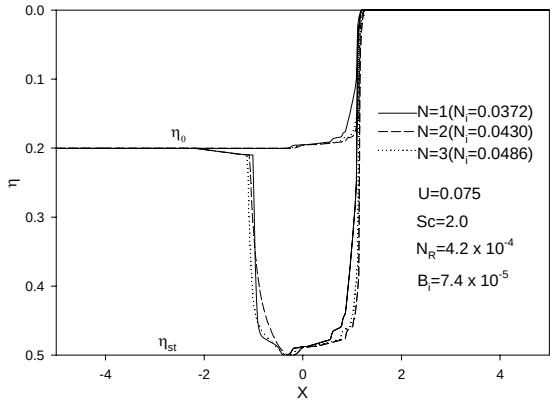

Fig. 4 Effects of numbers of existing sintered layers on the sintering process ($\Delta = 0.5$, $U = 0.075$)

The effect of the different numbers of the existing sintered layers on the sintering process of the loose powder layer ($\Delta = 0.5$) at $U = 0.075$ is shown in Fig. 4. The shape of the liquid pool at specific numbers of the existing sintered layers is similar to those in Fig. 2 but the volume of the liquid pool is larger. It is because that the laser beam intensity increases significantly in order to have the sintering depth outstrip the bottom surface of the loose powder layer compared with the sintering process in Fig. 2. The effect of the number of existing sintered layers on the sintering process in the loose powder layer at $U = 0.1$ is shown in Fig. 5. As we can see in Fig. 5, the liquid pool keeps the similar shape when the laser beam scanning velocity increases insignificantly. The numerical simulations are then performed for the effect of the different numbers of existing sintered layers on the sintering process at both $U = 0.075$ and $U = 0.1$ when the dimensionless thickness of the loose powder layer is 1.0 and the results are shown in Fig. 6-7. Similar trend compared with the corresponding case in Fig. 4-5 can also be observed.

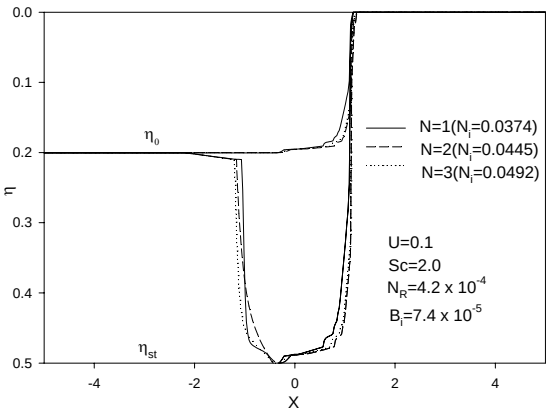

Fig. 5 Effects of numbers of existing sintered layers on the sintering process ($\Delta = 0.5$, $U = 0.1$)

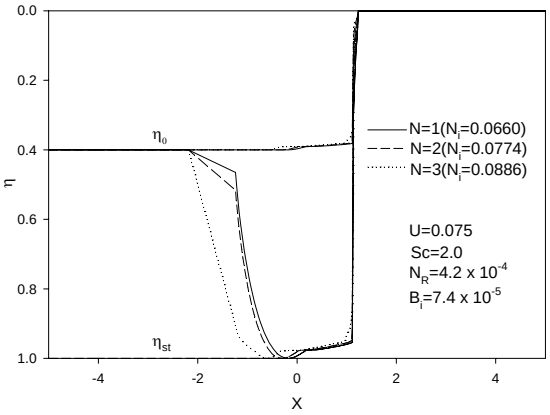

Fig. 6 Effects of numbers of existing sintered layers on the sintering process ($\Delta = 1.0$, $U = 0.075$)

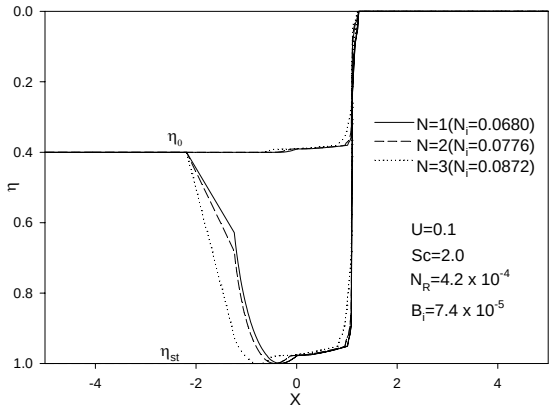

Fig. 7 Effects of numbers of existing sintered layers on the sintering process ($\Delta = 1.0$, $U = 0.1$)

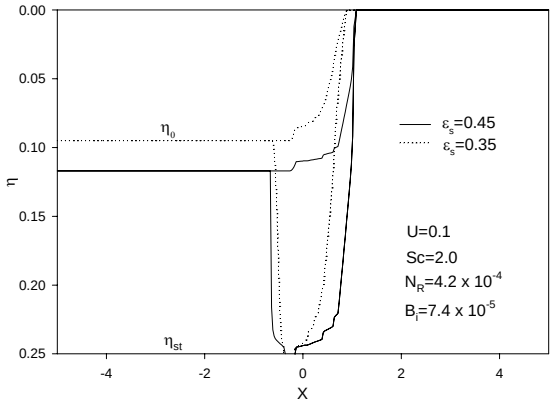

Fig. 8 Effects of numbers of existing sintered layers on the sintering process ($\Delta = 0.25$, $U = 0.1$, $N = 1$)

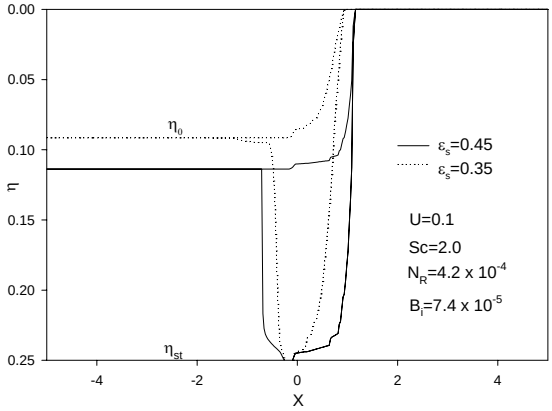

Fig. 9 Effects of numbers of existing sintered layers on the sintering process ($\Delta = 0.25$, $U = 0.1$, $N = 2$)

Figure 8 shows the effect of the porosity of the loose powder layer with one existing sintered layer on the sintering process. It can be seen that the shrinkage of the loose powder layer is increased significantly by

increasing the porosity since more gas is released from the loose powder layer when heated by the moving laser beam. The liquid pool for the larger porosity of the loose powder layer is wider than that at smaller porosity. That is due to the lower effective thermal conductivity of the loose powder layer with the larger porosity which reduces the dissipation of the heat flux and cause more melting happened. The effect of the porosity of the loose powder layer with two existing sintered layers below on the sintering process is shown in Fig. 9. Similar phenomena which were interpreted in Fig. 8 can be observed. However, the ripples on the top surface of the liquid pool are weakened compared with the corresponding case in Fig. 8 when the number of the existing sintered layers increases.

5. CONCLUSIONS

A numerical study of a two-dimensional SLS process in a loose powder layer with different thickness on top of the multiple sintered metal powder layers is presented. The results showed that the thickness of the loose powder layer can affect the formation of the liquid pool significantly in the sintering process. The optimized dimensionless moving heat source intensity increases with the increase of the thickness of the loose powder layer, the number of the existing sintered layers and the laser beam scanning velocity in order to achieve the desired sintering depth to bond the newly sintered layer to the existing sintered layer. Meanwhile, the porosity of the loose powder layer which plays the significant role in the sintering process needs to consider in the modeling process.

Acknowledgement: support for this work by the Office of Naval Research under grant number N00014-02-1-0356 is greatly acknowledged.

REFERENCES

Basu, B., and Srinivasan, J., 1988, "Numerical Study of Steady-State Laser Melting Problem," *Int. J Heat Mass Transfer*, Vol. 31, No.11, pp. 2331-2338.

Bunnell, D., 1995, *Fundamentals of Selective Laser Sintering of Metals*, Ph.D. Thesis, University of Texas at Austin.

Cao, Y. and Faghri, A., 1990, "A Numerical Analysis of Phase Change Problems Including Natural Convection," ASME *Journal of Heat Transfer*, Vol. 112, pp. 812-816.

Chan, C., Mazumder, J., and Chen, M., 1984, "A Two Dimensional Transient Model for Convection in Laser Melted Pool," *Metall. Trans*., Vol. 15A, pp. 2175-2184.

Chen, T., and Zhang, Y., 2003, "Analysis of Melting in a Mixed Powder Bed with Finite Thickness Subjected to Constant Heat Flux Heating," *Proceeding of ASME Summer Heat Transfer Conference*, Las Vegas, NV.

Chen, T., and Zhang, Y., 2003, "Two-Dimensional Modeling of Sintering of a Two-component Metal Powder layer on Top of Multiple Sintered Layers," *Proceedings of Solid Freeform Fabrication Symposium 2003*, pp.208-218, Austin, TX.

Conley, J., and Marcus, H., 1997, "Rapid Prototyping and Solid Freeform Fabrication," ASME *Journal of Manufacturing Science and Engineering*, Vol. 119, pp. 811-816.

Karapatics, N., Egger, G., Gygax, P.E., and Glardon, R., 1999, "Optimization of power Layer Density in Selective Laser Sintering," *Proceedings of Solid Freeform Fabrication Symposium 1999*, pp.255-263, Austin, TX.

Manzur, T., DeMaria, T., Chen, W., and Roychoudhuri, C., 1996, "Potential Role of High Powder Laser Diode in Manufacturing," presented at SPIE Photonics West Conference, San Jose, CA.

Patankar, S. V., 1980, *Numerical Heat Transfer and Fluid Flow*, McGraw-Hill, New York.

Storch, S., Nellessen, D., Schaefer, G., and Reiter, R., 2003, "Selective Laser Sintering: Qualifying Analysis of Metal Based Powder Systems For Automotive Application," *Rapid Prototyping Journal*, Vol.9, pp. 240-251.

Taylor, C.M., and Hauser, C., 2002, "Morphology of Direct SLS-Processed Stainless Steel Layers," *Proceedings of Solid Freeform Fabrication Symposium 2002*, pp.530-537, Austin, TX.

Viskanta, R., 1983, Phase Change Heat Transfer, in: G.A. Lane (Ed.), *Solar Heat Storage: Latent Heat Materials*, CRC Press, Boca Raton, FL.

Yao, L., and Prusa, J., 1989 "Melting and Freezing," *Advances in Heat Transfer*, Vol. 25, pp. 1-96, Academic Press, San Diego, CA..

Zhang, Y., and Faghri, A., 1998, "Melting and Resolidification of a Subcooled Mixed Powder Bed with Moving Gaussian Heat Source," ASME *Journal of Heat Transfer* Vol. 120, pp. 883-891.

Zhang, Y., and Faghri, A., 1999, "Melting of a Subcooled Mixed powder Bed with Constant Heat Flux Heating," *International Journal of Heat and Mass Transfer*, Vol. 42, pp. 775-788.

Zhang, Y., Faghri A., Buckley C.W., and Bergman T. L., 2000, "Three-Dimensional Sintering of Two-Component Metal Powders With Stationary and Moving Laser Beams," ASME *Journal of Heat Transfer*, Vol. 122, pp150-158.